Natural aging effect on the forming behavior of a cylindrical cup with an Al-Mg-Si alloy

V. Simões, H. Laurent, M. Oliveira, L. Menezes

Natural Aging Effect on the Forming Behavior of a Cylindrical Cup with an Al-Mg-Si Alloy

V.M. Simões[1, 2, a)], H. Laurent[1], M.C. Oliveira[2, c)], L.F. Menezes[2, c)]

[1]*Université de Bretagne-Sud, EA 4250, LIMATB, F-56100 Lorient, France*
[2] *CEMUC, Dep. de Eng. Mec., Univ. de Coimbra Polo II, Pinhal de Marrocos, 3030-788 Coimbra*

[a)]Corresponding author: vasco.simoes@univ-ubs.fr
[b)]herve.laurent@univ-ubs.fr
[c)]{marta.oliveira, luis.menezes}@dem.uc.pt

Abstract. Natural Aging of EN AW 6016-T4 is experimentally evaluated under uniaxial tensile test and forming of a cylindrical cup. The uniaxial tensile tests were performed 4 days, 1, 4, 7 and, 18 months after the alloy quenching. The results shows an increase of the proof and tensile strengths, while the in-plane anisotropy remains globally invariable with the increase of the storage time. The forming of cylindrical cups was performed too, with specimens at 1 and 18 months of natural aging. The increase of the proof and tensile strengths leads to an increase of the punch force during the deep drawing process. However, the effect on the thickness evolution along the cup's wall and on the cup's height is negligible. In fact, the numerical simulation results indicate that these parameters are more sensitive to the initial sheet thickness (considering the mean value of 1.047mm or the approximated one of 1.000mm) than to the changes induced by aging in the hardening behavior.

INTRODUCTION

Al-Mg-Si are frequently used Al-based alloys due to the good formability in non-aged state and, due to the possibility to be bake-hardened ("artificial aging" achieved by an age hardening at ≈180ºC during ≈30 min) to medium strength. Therefore, these alloys have many applications in transports industry, namely in automotive industry. Al-Mg-Si alloys are delivered in supersaturated states due to quenching, and may often present an increase of the proof and tensile strength, due to storage at room temperature. This effect, known as natural aging, occurs after quenching when the alloys are stored at room temperature (RT) during a time period (storage time). In general, natural aging is considered to be not relevant from the technological point of view for Al-Mg-Si alloys, since they are always submitted to artificial aging [1]. Nevertheless, natural aging is often analyzed in order to understand its "negative effect" in the subsequent bake hardening step, since it causes longer precipitates with a lower volume fraction. This leads to lower peak hardness and increased ductility after bake hardening [1]. During natural aging stage the proof strength ($R_{p0.2}$ [2]) and the tensile strength (R_m [2]) increases and ductility is reduced [3,4]. In fact, it has been proposed to represent the evolution of the $R_{p0.2}$ with the natural aging time (t_{NA}) using a logarithmic function, such that $R_{p0.2} = k \cdot \log(t_{NA}) + R_i$, where k is a natural aging kinetics parameter and R_i represents the initial yield strength of the alloy (after quenching and storage at room temperature for ≈1 h) [5-7].

Since it was first observed by Wilm in 1904 [8], the study of the age hardening behavior process has contributed greatly to the optimization of aluminum alloys performance. This complex process was first explained by Guinner and Preston in 1938 [9,10] for the Aluminum alloys and, later for Al-Mg-Si Alloys [11]. Nevertheless, the scientific knowledge about the mechanisms is still rather fragmentary due to the difficulties on its analysis [1,12]. In fact, the study of natural aging in 6000 series alloys is complicated because: firstly, the content of Mg and Si is always very low, i.e. 1.5 or 1.2wt% for each of the elements Si and Mg, respectively; secondly, Mg, Al, and Si are neighboring elements in the periodic table [1].

This work is focused on an EN AW 6016 alloy that is used in automotive industry and is expected to show superior formability and higher corrosion resistance with a low paint baked strength. The main goal is to understand the influence of natural aging on the forming behavior of this Al-Mg-Si alloys. Therefore, the natural aging was evaluated by performing tensile test at 1, 4, 7 and 18 months after quenching.

SELECTED MATERIAL AND EXPERIMENTAL PROCEDURE

The EN AW 6016-T4 alloy is known as a Si excess alloy since the Mg/Si ratio in mass fraction percentage [wt.%] is less than one. The sheets were made and supplied by Constellium with a Mg/Si ratio equal to 0.19 [wt.%] and were cold rolled up to 1.04mm thickness, annealed, quenched and natural aged (T4). The mechanical properties were evaluated by the supplier using uniaxial tensile tests, performed after 4 days of maturations at RT and are presented in Table 1.

TABLE 1. Mechanical properties of EN AW 6016-T4 (supplier results). R_m tensile strength. $R_{p0.2}$ proof strength at 0.2% of the extensometer gauge length. Ag percentage of non-proportional elongation at maximum force. $n_{4\text{-}6}$ strain hardening coefficient between 4 and 6 % of plastic elongation. $n_{10\text{-}15}$ strain hardening coefficient between 10 and 15 % of plastic elongation (terms and definitions according with the European Standard EN 10002-1 [2]).

R_m	$R_{p0.2}$	Ag	$n_{4\text{-}6}$	$n_{10\text{-}15}$
198 MPa	88 MPa	24.6 %	0.32	0.27

The static strain aging due to material storage at room temperature was evaluated using uniaxial tensile tests performed 1, 4, 7 and 18 months after the heat treatment. The strain rate of $2x10^{-3}s^{-1}$ was adopted as reference and used in all tests. At least two tensile tests were performed for each test condition and the results were always reproducible with an average scatter of true stress less than ±1MPa, for the same value of true strain. Thus, in the following section only the result of one of the tests is presented. The strain fields were measured by Digital Image Correlation (DIC) technique using ARAMIS 4M 3D optical system. The anisotropic behavior was analyzed for specimens with 1 and 7 months of storage time, by performing test with three different in-plane directions: 0°, 45° and 90° to rolling direction (RD).

The formability was evaluated using the cylindrical cup benchmark test, with the tools dimensions shown in Fig. 1 a). The circular blank with an initial diameter of 60 mm is radially drawn into the die by the punch movement (Fig. 1 b)) to obtain a cylindrical cup (Fig. 1 c)). The blank-holder force of 6 kN was selected in order to avoid wrinkles and the punch force is recorded during the test. The blank is lubricated with an Aerosol Oil Spray [13] in an amount which avoids the occurrence of galling.

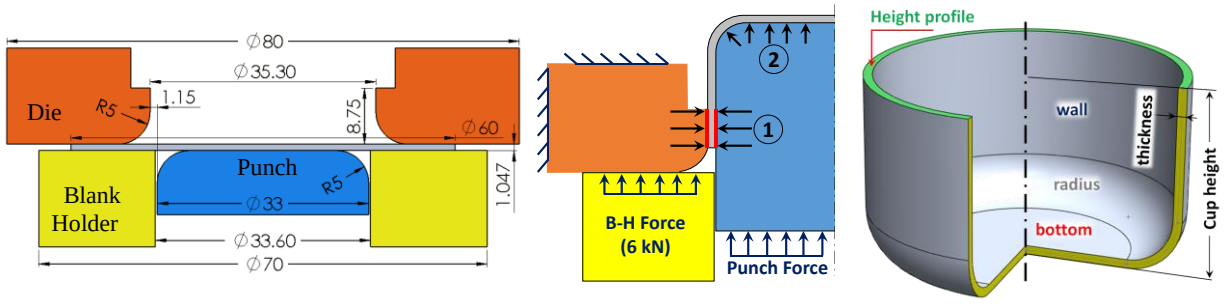

(a) (b) (c)

FIGURE 1. Deep drawing of a cylindrical cup: (a) Tools in initial position with dimensions; (b) Ironing phase; (c) Final cup geometry and its sections.

The cylindrical cup tests were performed in a Zwick BUP200 machine [14]. The cup thickness and height measurements (Fig. 1 c)) were performed using a 3D machine "Brown & Sharpe Mfg. Co.", model "MicroXcel PFX-454". The thickness is evaluated based on the coordinates measurements performed along the interior and the exterior sides of the cup, in a normal direction to the surface; the difference between the interior and exterior coordinates is the thickness value. The measurements were performed along several directions to the RD, such that the value presented corresponds to the average of the results obtained, as follows: 0º to RD (average of 0º and 180º); 45º to RD

(average of 45º, 135º, 225º and 315º); 90º to RD (average of 90º and 270º) [15]. The cup height is measured from 0º to 355º to RD with a step of 5º [15]. The cup height measurements are presented from 0º to 90º taking into account average the assumed cup symmetries. The results presented for the punch force, cup thickness and cup height are the average of the results obtained for the three cylindrical cup tests performed.

TENSILE TESTS RESULTS

The tensile test results obtained with specimens with different storage time are presented in Fig. 2. Figure 2 a) shows the influence of natural aging on the mechanical properties along the RD. Globally, natural aging leads to an increase of the yield and ultimate tensile stresses(or R_{02} and R_m) with the increase of the storage time [3,4], with a negligible influence in the hardening coefficient. In an initial period there is a fast increase of both R_{02} and R_m, which tends to stabilize for longer storage time periods. As previously mentioned, this behaviour can be described with a logarithmic function [5], as shown in Fig. 2 b) for the material under analysis.

Concerning the in-plane anisotropic behaviour, the results show a negligible influence of natural aging for both the flow stresses (see Fig. 2 c)) and the r-values (see Fig. 2 d)). Despite the small differences reported for the r-values, the trend is globally the same. Other works have also reported that this alloy keeps the same anisotropic trends despite the negligible influence of natural aging [3].

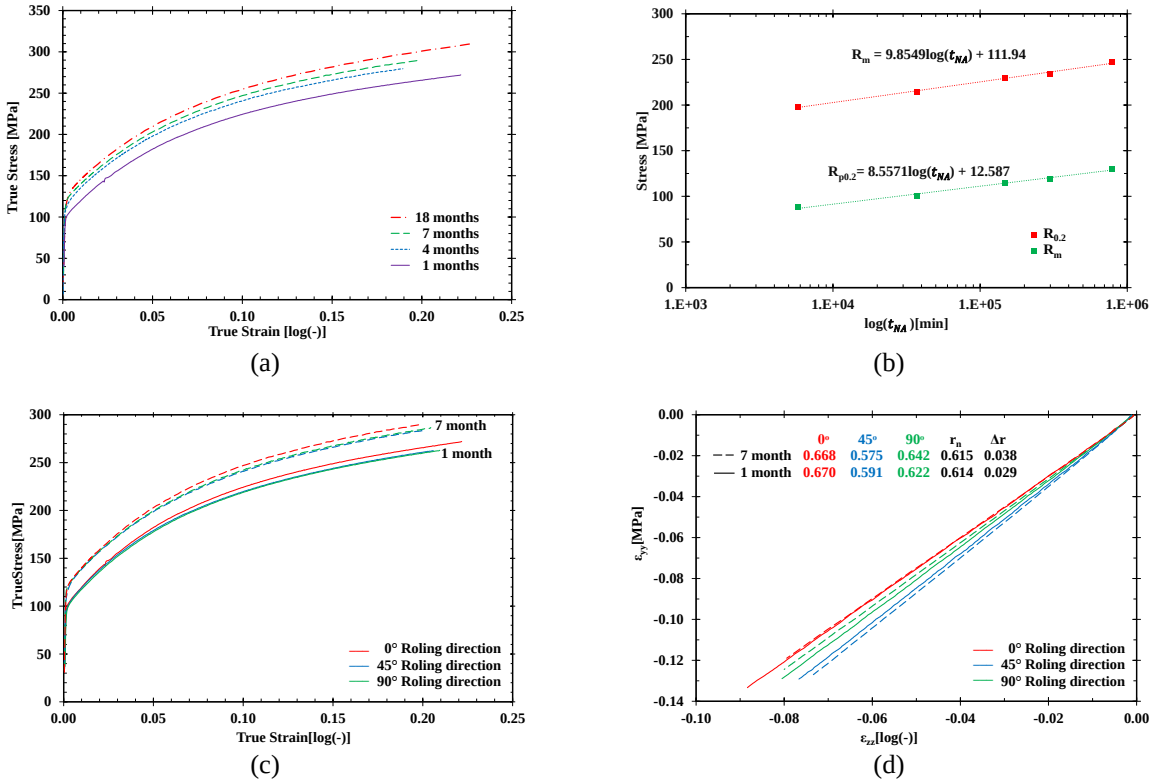

FIGURE 2. Natural aging effect on material behavior: a) Stress-strain curves along RD, obtained from uniaxial tensile tests performed at different storage time; b) Logarithmic evolution of the yield and ultimate tensile stresses with natural aging time (average of 6 test minimum including different anisotropic directions); Influence of natural aging on anisotropic behavior: c) stress-strain curves and d) r-values.

Based on this set of experimental results, the constitutive parameters for the isotropic hardening Voce law ($Y = Y_0 + (Y_{sat} - Y_0)[1 - \exp(-C_Y \bar{\varepsilon}^p)]$) [16] and the Barlat et al. (1991) yield criterion (YLD'91) [17] were identified using the in-house code DD3MAT [18], for 1 and 18 months of storage. It should be mentioned that in order to ameliorate the definition of the in-plane stress directionalities for the yield criterion parameters identification, the experimental values considered correspond to an equivalent plastic strain $\bar{\varepsilon}^p$ value of 5%. Also, it is assumed that the r-values remain unchanged after 7 months of storage time. The identified parameters are presented in Table 2.

TABLE 2. Parameters identified for the constitutive model adopted using the in-house code DD3MAT [18]

	Voce Law			**Yld91** (m=8)				
	Y_0	C_Y	Y_{sat}	C_1	C_2	C_3	C_4= C_5	C_6
1 months	109.9	11.58	280.9	1.1078	1.0866	0.9684	1	0.9917
18 months	131.4	12.08	312.3	1.0899	1.0699	0.9533	1	0.9758

FORMING TESTS RESULTS

Figure 3 presents the results obtained for the cylindrical cup tests performed with the sheet after a storage time of 1 and 18 months. Figure 3 a) presents the punch force evolution with punch displacement, highlighting the two distinct phases that occur during the process: drawing and ironing. The drawing phase involves the deformation up to ≈19mm of punch displacement, where a noticeable local minimum of the punch force occurs when the blank loses contact with the blank-holder. After that point the ironing phase starts, with an increase of the punch force until attaining a local maximum (≈23mm of punch displacement), followed by a decreases until the end of the process. Ironing occurs since the thickness of the blank is higher than the gap between the die and the punch (1.150mm). Therefore, the sheet is strongly compressed between the punch and die (see Fig. 1 b)), which typically imposes high contact forces, normal to the surface of the punch and the die. Globally, the results show an increase of the punch force with increasing aging time, which can be related with the increase of the flow stress presented in Fig. 2 a).

In order to better understand these experimental results, the numerical analysis of the cylindrical cup forming process was performed using the in-house code DD3IMP [19]. The blank is discretized with 3-D solid elements with 8 nodes. The tools are assumed to behave rigidly with the die modeled using Nagata surfaces [20] and the blank-holder and the punch with Bézier surfaces. The elastic regime assumes an isotropic behavior, described by the Young's modulus (E=69 [GPa]) and the Poisson ratio (ν=0.33). The constitutive model adopted for both specimens uses the parameters previously shown in Table 2. Regarding the sheet thickness, as previously mentioned, the supplier indicates a value of 1.04 mm. In fact, the average value obtained for more than 130 measurements was 1.047mm. Therefore, two models were considered: one with 1.000 mm and another with 1.047mm, of initial blank thickness. The friction is modelled with the Coulomb's law using a constant value of 0.15, since it allows a good reproduction of the punch force during the drawing phase, as shown in Fig. 3 a) for the 1.047mm thick blank.

Globally, the numerical simulation results for the drawing stage corroborate the influence of natural aging on the punch force evolution, i.e. the increase of the punch force associated to the increase of the flow stress. Figure 3 b) compares the punch force evolution for both specimens, as predicted by the models with different initial blank thicknesses. The results show that an increase of ≈0.05mm (≈5%) in the sheet thickness, globally, it has the same impact in the punch force during drawing as the increase of the flow stress due to natural aging.

The punch force evolution results clearly show that the ironing stage is not well predicted. Nevertheless, it should be mentioned that it is known that this stage is quite sensitive to the gap value between the punch and the die [21] (see Fig.1) as well as to the friction conditions [15,22]. In this context, Fig. 3 c) presents the thickness evolution along a curvilinear coordinate, corresponding to the distance to the cup's center. The profile of the thickness evolution clearly shows the two critical points where the minimum thickness value is typically obtained, corresponding to the begin and end of the punch radius [23]. Along the cup's wall, the thickness increases until attaining a constant value, which was imposed by the ironing stage. Thus, it is possible to confirm that the gap between the die and the punch is slightly higher in the experimental device than in the numerical model.

The experimental results indicate that natural aging has a negligible effect in the thickness evolution (Fig. 3 c)), which is corroborated by the numerical analysis. A slight decrease in thickness is observed for the material with 1 month of storage time, due to the lower flow stress value, in both experimental and numerical results. On other hand, the initial thickness of the blank used in the numerical simulation is a major factor to accurately predict thickness evolution. The results considering an initial thickness of 1.047mm show a very good agreement with the experimental ones. The small differences in the cup's bottom can be associated to the fact that the parameters for the YLD91 yield criterion were identified without any information regarding the equi-biaxial stress state behavior. In addition, the differences in the cup's wall can be related with the stronger ironing stage imposed by the numerical model, since this slope is influenced by the value for the maximum thickness allowed.

Figure 3 d) presents the cup's height profile which shows always the same trend: maxima at RD and TD and minimum at 45^0 to RD and equivalent positions. Thus, it can be stated that the ear profile is not influenced by natural aging, which is in agreement with the trend observed for the in-plane anisotropic behaviour in the uniaxial tensile tests. In the experimental results, the amplitude of the ears (difference between maximum and minimum height) is higher for the 18 months naturally aged material, which also seems to be in agreement with the slightly higher value for Δr (see Fig. 2 d)). The global cup's height is underestimated in the numerical simulations as a sequence of a smaller flow of the blank during the drawing step (loss of contact with the blank-holder occurs later). Although the numerical results obtained with an initial blank thickness of 1.047mm show a slightly higher profile, this seems to be caused by the strong stretching during the ironing stage.

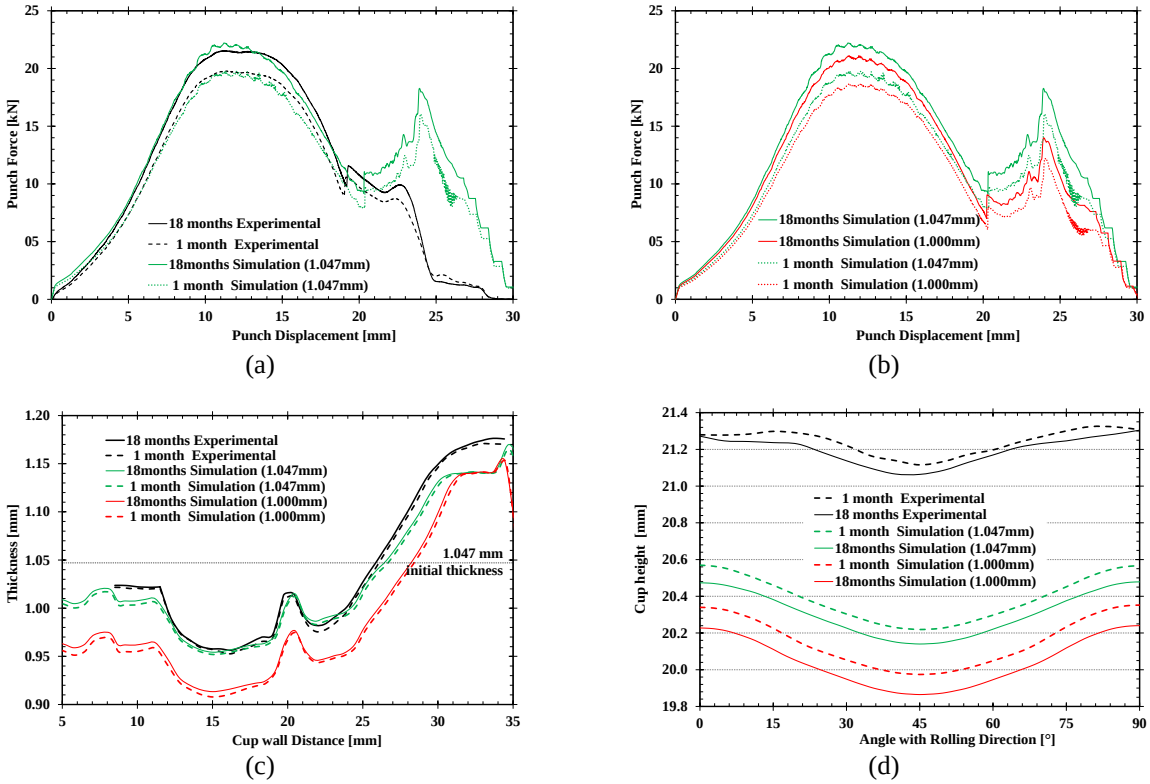

FIGURE 3. Results of the cylindrical cup forming:
Punch force evolution with punch displacement (a) Experimental results *vs* numerical results with a blank with an initial thickness of 1.047mm, for 1 and 18 months of storage time, (b) Numerical results with blanks with initial thickness of 1.000mm and 1.047mm, for 1 and 18 months of storage time;
Experimental results vs Numerical results with blanks with initial thickness of 1.000mm and 1.047mm, for 1 and 18 months of storage time: (c) Thickness evolution along the cup's and (d) Cup's height.

Summary:

A study on the natural aging effect on EN AW 6016-T4 formability was performed. The alloy shows a logarithmic increase of the proof and tensile strength with storage time increase. The anisotropic behavior is negligible influenced by the natural aging, which leads to minor variations of the thickness evolution along the cup's profile and also of the cup's height. Thus, although there is a slight increase of the force needed to deform the blank this is not a relevant factor from an industrial point of view. The numerical simulation results highlight the importance of the accuracy in the initial blank thickness, in order to be able to predict accurate distributions for this parameter, which is often used to evaluate the constitutive models performance.

ACKNOWLEDGMENTS

This research work is sponsored by national funds from the French Ministry of Higher Education and the Portuguese Foundation for Science and Technology (FCT) via the project PTDC/EMS-TEC/1805/2012 and by FEDER funds through the program COMPETE – Programa Operacional Factores de Competitividade, under the project CENTRO -07-0224 -FEDER -002001 (MT4MOBI). The authors are also grateful to Constellium for supplying the material to perform the experimental tests. The first author is also grateful to the FCT for the PhD grant SFRH/BD/90669/2012.

REFERENCES

1. J. Banhart, C.S.T. Chang, Z. Liang, N. Wanderka, M.D.H. Lay, and A.J. Hill, Adv. Eng. Mater. **12**, 559 (2010).
2. Central Secretariat ISO, *ISO 6892-1:2009 Metallic Materials - Tensile Testing - Part 1: Method of Test at Room Temperature* (International Organization for Standardization, 2009), p. 65.
3. A. Mishra, Experimental Investigation and Numerical Prediction of Rupture in Bending of Metallic Sheets, Université de Bretagne-Sud, 2013.
4. A. Cuniberti, A. Tolley, M.V.C. Riglos, and R. Giovachini, Mater. Sci. Eng. A **527**, 5307 (2010).
5. S. Esmaeili and D.J. Lloyd, Scr. Mater. **50**, 155 (2004).
6. S. Esmaeili, D.J. Lloyd, and W.J. Poole, Acta Mater. **51**, 3467 (2003).
7. S. Esmaeili and D.J. Lloyd, Acta Mater. **53**, 5257 (2005).
8. A. Wilm, Metall. Z. Für Gesamte Hüttenkd. **8**, 225 (1911).
9. André Guinier, Nature **142**, 569 (1938).
10. G. D. Preston, Nature **142**, 570 (1938).
11. P. Brenner and H. Kostron, Z Met. **4**, 89 (1939).
12. L. Ding, Z. Jia, Z. Zhang, R.E. Sanders, Q. Liu, and G. Yang, Mater. Sci. Eng. A **627**, 119 (2015).
13. Jelt Grease 5411 aerosol 95cSt.
14. H. Laurent, J. Coër, P.Y. Manach, M.C. Oliveira, and L.F. Menezes, Int. J. Mech. Sci. **93**, 59 (2015).
15. J. Coër, Mise En Forme Par Emboutissage En Température D'un Alliage D'aluminium AA5754-O, Université de Bretagne Sud, 2013.
16. E. Voce, J. Inst. Met. **537** (1948).
17. F. Barlat, D.J. Lege, and J.C. Brem, Int. J. Plast. **7**, 693 (1991).
18. J. L. Alves, M.C. Oliveira, and L.F. Menezes, in *AIP Conf. Proc.*, **712**, 1645 (2004).
19. L.F. Menezes and C. Teodosiu, J. Mater. Process. Technol. **97**, 100 (2000).
20. D.M. Neto, M.C. Oliveira, L.F. Menezes, and J.L. Alves, Comput.-Aided Des. **45**, 639 (2013).
21. V.M. Simões, Analysis of the Influence of Process Parameters in the Deep Drawing of a Cylindrical Cup, Universidade de Coimbra, 2012.
22. V.M. Simões, J. Coër, H. Laurent, M.C. Oliveira, J.L. Alves, P.Y. Manach, and L.F. Menezes, Key Eng. Mater. **554-557**, 2256 (2013).
23. M. Colgan and J. Monaghan, J. Mater. Process. Technol. **132**, 35 (2003).